

D. Canbula^{1*}, B. Canbula²¹ Department of Alternative Energy Resources Technology, Manisa Celal Bayar University, Manisa, Turkey² Department of Computer Engineering, Manisa Celal Bayar University, Manisa, Turkey

*Corresponding author: deniz.canbula@cbu.edu.tr

**CROSS-SECTION CALCULATIONS OF PHOTOFISSION REACTIONS
FOR ^{238,239,240,241,242,244}Pu ISOTOPES USING NUCLEAR LEVEL DENSITY**

Photofission cross-sections of ^{238,239,240,241,242,244}Pu isotopes are theoretically investigated with the collective semi-classical Fermi gas model (CSCFGM) by using Talys computer code in the energy range 1 - 30 MeV. Nuclear level density has significant importance to define the structural properties of nuclei. CSCFGM is a nuclear level density model, that includes collective (rotational and vibrational) effects as well as the pairing and shell effects, and is used to analyse the (γ , f) reactions of plutonium isotopes. The experimental data for all reactions are taken from EXFOR library. The theoretical predictions are in agreement with the experimental data, Talys code without changing the input, and the evaluated nuclear cross-section data from TENDL 2021 library.

Keywords: photofission reaction, Talys, nuclear level density, plutonium isotopes.

1. Introduction

With developing technology and increasing energy deficit, it is started to think more about the energy sources in all countries. Energy sources are increasingly important to protect the natural balance of the world. One of the energy sources, nuclear energy is actually known to be safer and environmentally friendly when compares with other power plants and is extensively produced from the fission of uranium and plutonium. Therefore, nuclear reactions of actinides such as uranium and plutonium have special importance. Especially, nuclear data of gamma-induced reactions of these isotopes can be used in radiation transport simulation, shielding of plasma in fusion reactors, activation analysis, and nuclear waste transmutation [1]. For all these applications, it is highly considered to be able to exactly obtain cross-sections where experimental data are nonexistent. Therefore, nuclear reaction models are required to obtain the reaction cross-sections, particularly at the unknown parts of the experimental data [2, 3].

Plutonium can be splitted, stored, and used again in recycled fuel for nuclear power plants and has many isotopes like all other heavy elements. All of them are radioactive because they are unstable, therefore, decay, emit particles, and some gamma radiation. ²³⁸Pu is a highly toxic isotope but is used as an energy source in medical applications and space technology [4, 5]. It is a high specific activity alpha emitter and has a half-life of 87.7 yrs. The first measurement of photofission cross-section of ²³⁸Pu is performed by Kapitza et. al up to 8 MeV gamma energy in 1969 [6]. Since then, many experimental

works have been carried out [7 - 9]. The most common isotope of plutonium, ²³⁹Pu emits energetic alpha particles and has a half-life of $2.41 \cdot 10^4$ yrs, so changes happen slowly in this isotope. It is used as a fuel in nuclear power reactors. There are lots of experimental works for photofission cross-section measurements of ²³⁹Pu up to 18 MeV incident energy in the literature [7, 10 - 17]. The heavier isotopes of plutonium, ²⁴⁰Pu, and ²⁴²Pu are long-lived alpha emitters and have half-lives of 6560 and 376000 yrs, respectively. ²⁴⁰Pu is the second most abundant plutonium isotope (after ²³⁹Pu). ²⁴²Pu has the second-longest half-life (after ²⁴⁴Pu) and its abundance is low. ²⁴²Pu is usually used as a spike, because it generally exists as a minor ingredient in plutonium of the nuclear fuel cycle. Gamma-induced fission reaction measurements of ²⁴⁰Pu and ²⁴²Pu have been performed over the years by some groups [6, 9, 18, 19]. ²⁴¹Pu is a short-lived beta emitter and has a half-life of 13.2 yrs to produce ²⁴¹Am and the amount of ²⁴¹Am increases in ²⁴¹Pu with time. The radiation measurements of these isotopes are important because the amount of Am in a sample relative to the amount of Pu can give information about the age of the material [20]. Some experimental works [11, 12, 15] exist for photofission reactions of ²⁴¹Pu in the literature. The last plutonium isotope for this work, ²⁴⁴Pu has the longest half-life (82 My), so is ideally suitable for dating the events which happen during that time. Unlike the other isotopes of plutonium, ²⁴⁴Pu is not produced by neutron capture reactions but occurs in nature only in trace amounts [21]. Only one experimental work exists for the photofission reaction of ²⁴⁴Pu [22]. There is a special interest to investigate

the fission of these isotopes using gamma rays due to the remarkable properties of plutonium isotopes. In this work, photofission cross-sections of plutonium isotopes are investigated up to 30 MeV gamma energy. Collective semi-classical Fermi gas model (CSCFGM) is used to reproduce the experimental data.

In the following of this paper: In Sec. 2, we give the method used in our calculations. In Sec. 3, we represent our results and their discussions. Finally, in Sec. 4, we present some concluding remarks.

2. Theory

2.1. Calculation method

One of the commonly used computer programs is Talys [23], which is a computer code system for the estimation and analysis of nuclear reactions. This computer program simulates the nuclear reactions which are caused by particles such as neutron, proton, deuteron, alpha, triton, and gamma ray in the energy range from 1 keV to 1 GeV. Additionally, several nuclear level density models can be used as an optional input in Talys.

The distribution of exciting levels of nuclei is a characteristic property. Discrete and continuous structures of these levels give us information about the deformation, shell, and pairing effects of nuclei. Exciting levels have a discrete distribution at low excitation energies but have a continuous distribution at increasing energies. One needs particularly to define these levels at increasing energies, with a nuclear level density function.

Nuclear level density studies have begun by Bethe [24] and continued with different approaches by some scientists [25 - 35] from 1937 until today. The Fermi gas model proposed by Bethe is basically used for all nuclear level density models because it is the simple and successful model for reproducing the experimental data. According to this model, nucleus consists of nucleons, which do not interact with each other, and so all of the excited levels are accepted to be formed by single-particle excitations and distributed with equal spacings. Nuclear level density is the number of the excited levels in uniting energy interval and its formulation is given as

$$\rho(U, J, \Pi) = \frac{1}{2} \frac{2J+1}{2\sqrt{2\pi}\sigma^3} \exp\left[-\frac{(J+1/2)^2}{2\sigma^2}\right] \frac{\sqrt{\pi}}{12} \frac{\exp[2\sqrt{aU}]}{a^{1/4}U^{5/4}}, \quad (1)$$

where J is a certain total angular momentum, Π is the parity and $\sigma^2 = TI/\hbar^2$ is the spin-cut off parameter described in terms of the nuclear

temperature $T = \sqrt{U/a}$ and the moment of inertia I , $U = E_x - \Delta$ is effective excitation energy and a is the level density parameter [24, 36]. Under an approach of coupling the total angular momentum projections, Eq. (1) summing by all spins and parities yields the total Fermi gas level density,

$$\rho^{tot}(U) = \frac{1}{12\sqrt{2}\sigma} \frac{\exp[2\sqrt{aU}]}{a^{1/4}U^{5/4}}. \quad (2)$$

Eq. (2) is only used in this place. a is the main variable of the level density function and the dependence of this parameter on the deformation parameter β and excitation energy U is provided by the Laplace-like formula (CSCFGM) [37],

$$a(U, \beta) = \tilde{a} \left(1 + A_c \frac{S_n}{U} \frac{\exp(-|U - E_0|/\sigma_c^3)}{\sigma_c^3} \right). \quad (3)$$

where S_n is the neutron separation energy, $E_0 = 0.2\hbar\omega$ is the first phonon state energy [38], $\hbar\omega = 41/A^{1/3}$ MeV and $\sigma_c^3 = \sigma_c^3/\tilde{a}$ is the scale parameter. The important input parameters for Talys used in the calculations are given in Table.

Default input parameters for Talys taken from RIPL-3 [41]

Z	A	S_n , MeV	U, MeV	\tilde{a} , 1/MeV
94	239	5.646	0.487	23.17571
94	240	6.534	1.137	23.13066
94	241	5.242	0.404	23.25101
94	242	6.310	1.084	23.98803

A_c is the collective amplitude and presents the shape (and thus the deformation) dependence on the level density parameter and is given below

$$A_c = S(N, Z, T_c, Shape) = \left[M_{exp} - M_{LDM} \right] \frac{\tau_c}{\sinh\tau_c}, \quad (4)$$

$T_c = \sqrt{S_n/\tilde{a}}$ is the critical temperature and $\tau_c = 2\pi^2 T_c/\hbar\omega$. M_{exp} is the experimental mass of the nucleus and $M_{LDM} = M_0 + E\theta^2$ is the calculation of the deformed nucleus with the finite-range liquid-drop model [39]. M_0 is the calculated mass of the spherical nucleus having the same N and Z as the deformed nucleus. E is a coefficient defined in terms of parameter x which is a scale of the fission

capability of a nucleus and is given as $E = (2/5)c_2 A^{(2/3)}(1-x)\alpha_0^2$. $\alpha_0^2 = 5(a/r_0)A^{(-2/3)}$ and $\theta = \alpha/\alpha_0$ is the deformation magnitude and α is given in terms of the deformation parameter as $\alpha^2 = (5/4\pi)\beta^2$ [39].

Moreover, the asymptotic level density parameter \tilde{a} is used in terms of the single-particle level density at Fermi energy of the nucleus including the shell and pairing corrections [40]

$$\tilde{a} = \frac{\pi^2}{6} \sum_{i=p,n} g_i (E_f^i + S(N, Z, T_c, Shape) - \Delta), \quad (5)$$

where g is the single-particle level density and E_f is the Fermi energy. Shell correction $S(N, Z) = M_{exp}(N, Z) - M_{LDM}(N, Z, \beta = 0)$ and the pairing correction $\Delta = \pm 12/\sqrt{A}$ are taken into account.

3. Results and discussion

In this study, $^{238,239,240,241,242,244}\text{Pu}(\gamma, f)$ reaction cross-sections are calculated by using Talys computer code in the energy range from 1 to 30 MeV. The results compared with the experimental data taken from EXFOR library, Talys with default parameters [23] and TENDL 2021 library [42] are shown in Figs. 1 - 6. The cross-section calculations are performed for all reactions with CSCFGM.

3.1 $^{238}\text{Pu}(\gamma, f)$ reaction

Comparison of predicted results with the experimental data measured by some groups [6 - 9] for $^{238}\text{Pu}(\gamma, f)$ photofission reaction is given in Fig. 1. The reaction energy interval is 5 - 30 MeV. In this energy interval, cross-section values start from very low values and increase above 100 MeV. It is observed that all experimental works have close results. The theoretical result obtained with CSCFGM is presented in good agreement with all experimental data.

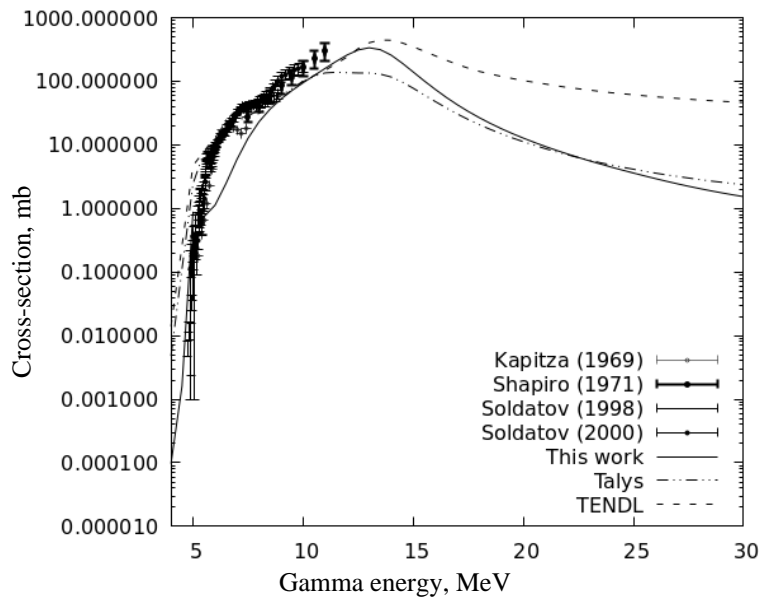


Fig. 1. $^{238}\text{Pu}(\gamma, f)$ photofission reaction cross-section calculation and comparison with the experimental data [6 - 9].

3.2 $^{239}\text{Pu}(\gamma, f)$ reaction

In Fig. 2, $^{239}\text{Pu}(\gamma, f)$ photofission reaction cross-section calculation result and comparison with the experimental data [7, 10 - 15, 17] are shown. There are many experimental works and experimental data are spread over a fairly wide range of cross-section values. The obtained result with CSCFGM is close to the existing data between 7 - 11 MeV.

3.3 $^{240}\text{Pu}(\gamma, f)$ reaction

The theoretically calculated cross-section and experimental data for $^{240}\text{Pu}(\gamma, f)$ [6, 9, 17] are repre-

sented in Fig. 3. There are three experimental works and one of them has a large experimental error. The vast majority of experimental data are in the energy range of 5 - 30 MeV. The calculated result with CSCFGM presents the overall distribution of the cross-section according to the gamma energy.

3.4 $^{241}\text{Pu}(\gamma, f)$ reaction

Fig. 4 shows the comparison between the calculated cross-section of $^{241}\text{Pu}(\gamma, f)$ and experimental data [11, 12, 15]. These data are close to each other. Theoretical prediction and experimental data are in agreement, especially after 7 MeV.

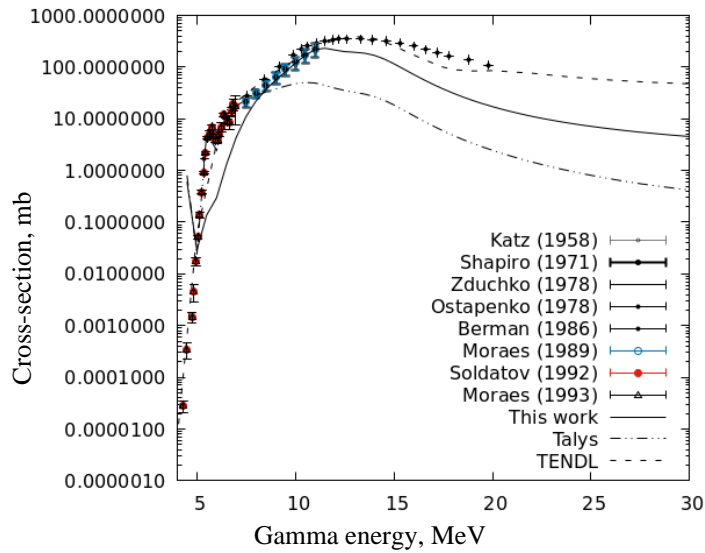


Fig. 2. $^{239}\text{Pu}(\gamma, f)$ photofission reaction cross-section calculation and comparison with the experimental data [7, 10 - 15, 17].

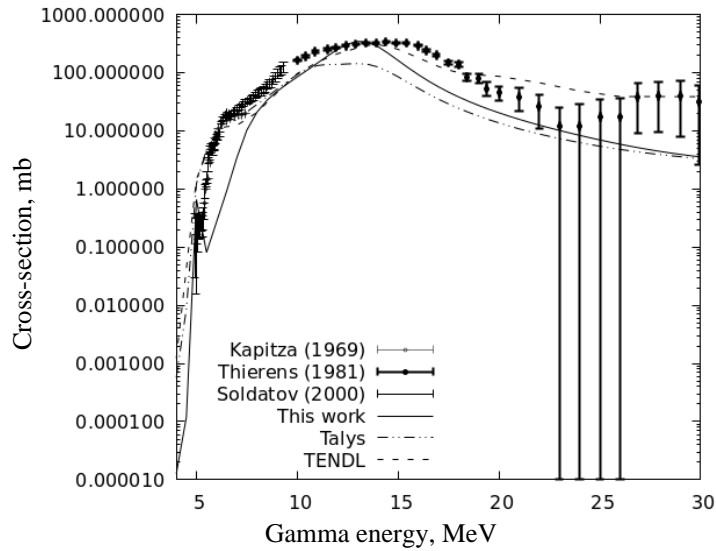


Fig. 3. $^{240}\text{Pu}(\gamma, f)$ photofission reaction cross-section calculation and comparison with the experimental data [6, 9, 17].

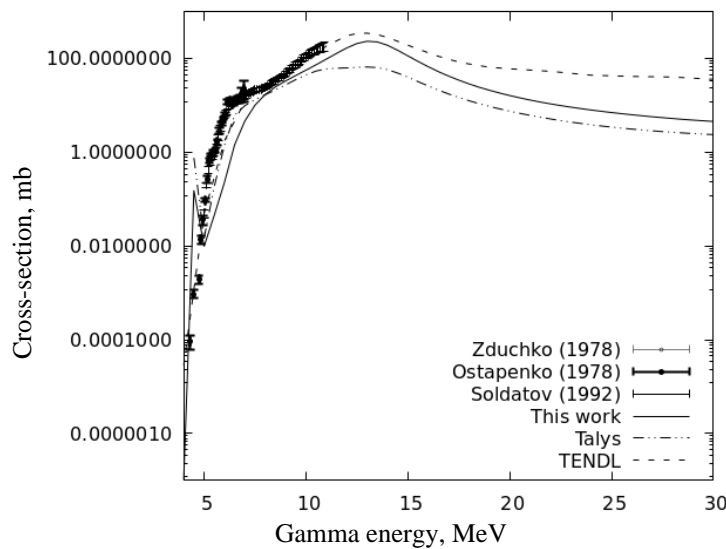


Fig. 4. $^{241}\text{Pu}(\gamma, f)$ photofission reaction cross-section calculation and comparison with the experimental data [11, 12, 15].

3.5 $^{242}\text{Pu}(\gamma, f)$ reaction

A comparison of the experimental cross-section values [6, 9, 18] with theoretical prediction based on the CSCFGM for $^{242}\text{Pu}(\gamma, f)$ is given in Fig. 5. All data values dramatically increase in the energy range of

5 - 10 MeV. One of the experimental works has a large experimental error. As seen from the Figure, theoretical prediction is in good agreement with the experimental data, but around 15 - 30 MeV, the prediction result moves away a little bit from the data values.

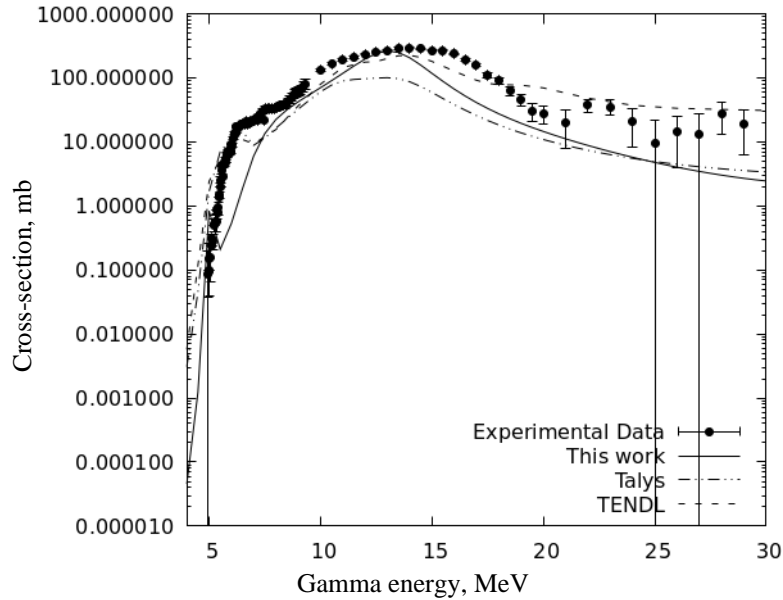


Fig. 5. $^{242}\text{Pu}(\gamma, f)$ photofission reaction cross-section calculation and comparison with the experimental data [6, 9, 18].

3.6 $^{244}\text{Pu}(\gamma, f)$ reaction

The calculation result with CSCFGM by using Talys code and comparison with experimental data [21] for $^{244}\text{Pu}(\gamma, f)$ are presented in Fig. 6. Only one experimental work is reported in the literature.

Experimental values start increasing from very high cross-section values according to other reactions. The CSCFGM result generally is consistent with the experimental data. However, experimental data have fluctuations in the energy range of 20 - 30 MeV, but theoretical prediction has not a similar behavior.

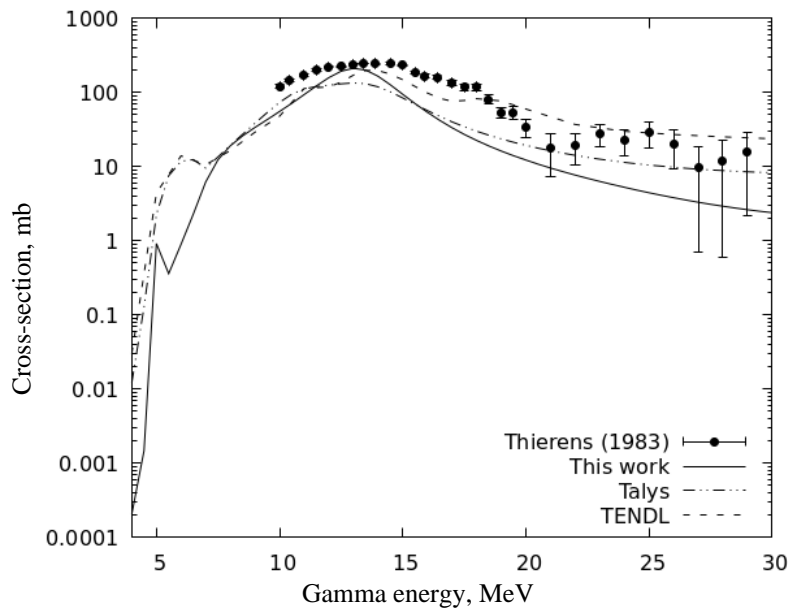


Fig. 6. $^{244}\text{Pu}(\gamma, f)$ photofission reaction cross-section calculation and comparison with the experimental data [22].

4. Conclusions

This study represents the results of theoretical model calculations of photofission reaction cross-sections of plutonium isotopes. The obtained theoretical results of (γ , f) reactions are performed with CSCFGM by using Talys computer code in the energy range 1 - 30 MeV and are compared with available experimental data in the literature. The results can be summarized as follows:

- The computed results with CSCFGM show the close results to the the measured data for all energy ranges not as much as TENDL and Talys results. However, this model can be used as an optional input. In addition, while unsmooth behavior around 5 MeV is observed at higher cross-section values in the experimental data, it is observed at lower cross-

section values in the calculation results. This behavior can partially be explained by the decreasing of shell corrections near the $N = 82$ mass region.

- CSCFGM provides the general behavior in the photofission reaction cross-section calculations of plutonium isotopes with the Talys code without changing the input in the program and TENDL 2021 library [42]. In addition, calculations from TENDL library are given with the best input parameters using Talys code. Therefore, the most reliable values of the cross-sections are presented from TENDL library.

- In this study, it is desired to show that a nuclear level density model which incorporates the collective effects into calculations more fundamentally, contrary to the general belief, can also be used in the calculations of nuclear reaction cross-section.

REFERENCES

1. Handbook on Photonuclear Data for Applications Cross Sections and Spectra. Final Report of a Co-ordinated Research Project 1996 - 1999. IAEA-TECDOC-1178 (Vienna: IAEA, 2000) 284 p.
2. B. Canbula. Collective effects in deuteron induced reactions of aluminum. *Nucl. Inst. Meth. B* 391 (2017) 73.
3. D. Canbula. Cross section analysis of proton-induced nuclear reactions of thorium. *Nucl. Inst. Meth. B* 478 (2020) 229.
4. D.L. Clark et al. Plutonium. In: *The Chemistry of the Actinide and Transactinide Elements*. L.R. Morss, N.M. Edelstein, J. Fuger (Eds). Ch. 7 (Netherlands: Springer, 2016) p. 813.
5. V.S. Mallela, V. Ilankumaran, N.S. Rao. Trends in cardiac pacemaker batteries. *Indian Pacing Electro-physiol. J.* 4(4) (2004) 201.
6. S.P. Kapitza et al. Photofission of even-even nuclei and structure of the fission barrier. *JETP Lett. (USSR) (Eng. transl.)* 9 (1969) 73.
7. A. Shapiro, W.F. Stubbins. Photofission cross section of plutonium-238 and plutonium-239. *Nucl. Sci. Eng.* 45(1) (1971) 47.
8. A.S. Soldatov. Photofission cross-section of plutonium-238, plutonium-240 and plutonium-242 in the energy region from 5 to 10 MeV. In: *Progress report. January 1997 - December 1998*. B. Kuzminov (Ed.) INDC(CCP)-420 (Russian Federation, Obninsk, 1998) p. 31.
9. A.S. Soldatov et al. Photofission of ^{238}Pu , ^{240}Pu , and ^{242}Pu in the energy range 5 - 10 MeV. *Phys. At. Nucl.* 63 (2000) 31.
10. L. Katz, A.P. Baerg, F. Brown. Photofission in heavy elements. A/CONF. 15/P/200. (Chalk River, Ontario, Atomic Energy of Canada Ltd., 1958).
11. V.E. Zhuchko et al. Investigation of probability of Th, U, Np, Pu, Am isotope fission near threshold by bremsstrahlung gamma quanta. *Yadernaya Fizika (USSR)* 28(5) (1978) 602.
12. Yu.B. Ostapenko et al. Yields and Cross Sections of Photofission for Isotopes Th, U, Np, and Am in Energy Range from 4.5 MeV to 7.0 MeV. *Voprosy Atomnoy Nauki i Tekhniki. Seriya Yadernye Konstanty* 3 (1978) 3.
13. B.L. Berman et al. Photofission and photoneutron cross sections and photofission neutron multiplicities for ^{233}U , ^{234}U , ^{237}Np , and ^{239}Pu . *Phys. Rev. C* 34(6) (1986) 2201.
14. M. Antonio, P.V. De Moraes. M.F. Cesar. Photofission cross sections of ^{233}U and ^{239}Pu near threshold induced by gamma rays from thermal neutron capture. *Nucl. Inst. Meth. A* 277 (1989) 467.
15. A.S. Soldatov, G.N. Smirenkin. Results of relative measuring of photofission yields and cross sections for nuclei $^{233,235}\text{U}$, ^{237}Np , $^{239,241}\text{Pu}$ and ^{241}Am in the energy region 5 - 11 MeV. *Yadernaya Fizika (USSR)* 55 (1992) 3153.
16. A.S. Soldatov, G.N. Smirenkin. Yield and cross section for fission of odd nuclei by γ rays with energies up to 11 MeV. *Phys. At. Nucl.* 55 (1992) 1757.
17. M. Antonio, P.V. De Moraes. M.F. Cesar. Photofission cross sections of Pu-239 using neutron capture gamma rays, near threshold. *Physica Scripta* 47(4) (1993) 519.
18. H. Thierens et al. Kinetic energy and fragment mass distributions for $^{240}\text{Pu}(s.f.)$, $^{239}\text{Pu}(n_{th}, f)$, and $^{240}\text{Pu}(\gamma, f)$. *Phys. Rev. C* 23(5) (1981) 2104.
19. H. Thierens et al. Fragment mass and kinetic energy distributions for $^{242}\text{Pu}(sf)$, $^{241}\text{Pu}(n_{th}, f)$, and $^{242}\text{Pu}(\gamma, f)$. *Phys. Rev. C* 29(2) (1984) 498.
20. M. Wallenius, K. Mayer. Age determination of plutonium material in nuclear forensics by thermal ionisation mass spectrometry. *Fresenius J. Anal. Chem.* 366(3) (2000) 234.
21. S.R. Winkler et al. Anthropogenic ^{244}Pu in the environment. *New Astronomy Reviews* 48(1-4) (2004) 151.
22. H. Thierens et al. Kinetic energy and fragment mass distributions for the spontaneous and photon-induced fission of ^{244}Pu . *Phys. Rev. C* 27(3) (1983) 1117.
23. A.J. Koning, S. Hilaire, M.C. Duijvestijn. TALYS-1.0. In: *Int. Conf. on Nucl. Data for Sci. and Techn.*,

- Nice, France, April 22 - 27, 2007 (EDP Sciences, 2007) p. 211.
24. H.A. Bethe. Nuclear physics B. Nuclear dynamics, theoretical. *Rev. Mod. Phys.* 9 (1937) 69.
 25. P. Demetriou, S. Goriely. Microscopic nuclear level densities for practical applications. *Nucl. Phys. A* 695 (2001) 95.
 26. W. Dilg et al. Level density parameters for the back-shifted Fermi gas model in the mass range $40 < A < 250$. *Nucl. Phys. A* 217(2) (1973) 269.
 27. A. Gilbert, A.G.W. Cameron. A composite nuclear-level density formula with shell corrections. *Can. J. Phys.* 43(8) (1965) 1446.
 28. S. Hilaire, S. Goriely. Global microscopic nuclear level densities within the HFB plus combinatorial method for practical applications. *Nucl. Phys. A* 779 (2006) 63.
 29. J.A. Holmes et al. Tables of thermonuclear-reaction-rate data for neutron-induced reactions on heavy nuclei. *At. Data Nucl. Data Tables* 18 (1976) 305.
 30. B. Krusche, K.P. Lieb. Dipole transition strengths and level densities in $A \leq 80$ odd-odd nuclei obtained from thermal neutron capture. *Phys. Rev. C* 34(6) (1986) 2103.
 31. B. Nerlo-Pomorska et al. Nuclear level densities within the relativistic mean-field theory. *Phys. Rev. C* 66(5) (2002) 051302.
 32. B. Nerlo-Pomorska, K. Pomorski. Pairing energy obtained by folding in the nucleon number space. *Int. J. Mod. Phys. E* 15(2) (2006) 471.
 33. B. Nerlo-Pomorska, K. Pomorski, J. Bartel. Shell energy and the level-density parameter of hot nuclei. *Phys. Rev. C* 74(3) (2006) 034327.
 34. T.D. Newton. Shell effects on the spacing of nuclear levels. *Can. J. Phys.* 34(8) (1956) 804.
 35. T. Von Egidy, H.H. Schmidt, A.N. Behkami. Nuclear level densities and level spacing distributions: Part II. *Nucl. Phys. A* 481 (1988) 189.
 36. T. Ericson. The statistical model and nuclear level densities. *Advan. Phys.* 9(36) (1960) 425.
 37. B. Canbula et al. A Laplace-like formula for the energy dependence of the nuclear level density parameter. *Nucl. Phys. A* 929 (2014) 54.
 38. A. Bohr, B.R. Mottelson. *Nuclear structure. Vol. 1* (London: World Scientific, 1998) 492 p.
 39. W.D. Myers, W.J. Swiatecki. Nuclear Masses and Deformations. *Nucl. Phys.* 81 (1966) 1.
 40. B. Canbula et al. Effects of single-particle potentials on the level density parameter. *Eur. Phys. J. A* 50 (2014) 178.
 41. R. Capote et al. RIPL - Reference Input Parameter Library for Calculation of Nuclear Reactions and Nuclear Data Evaluations. *Nucl. Data Sheets* 110(12) (2009) 3107.
 42. A.J. Koning et al. TENDL: Complete Nuclear Data Library for Innovative Nuclear Science and Technology. *Nucl. Data Sheets* 155 (2019) 1.

Д. Канбула^{1,*}, Б. Канбула²

¹ Факультет технологій альтернативних енергетичних ресурсів,
Університет Маніси Челал Баяр, Маніса, Туреччина

² Факультет комп'ютерної інженерії, Університет Маніси Челал Баяр, Маніса, Туреччина

*Відповідальний автор: deniz.canbula@cbu.edu.tr

РОЗРАХУНКИ ПОПЕРЕЧНИХ ПЕРЕРІЗІВ РЕАКЦІЙ ФОТОПОДІЛУ ДЛЯ ІЗОТОПІВ ^{238,239,240,241,242,244}Pu З ВИКОРИСТАННЯМ ГУСТИНИ ЯДЕРНИХ РІВНІВ

Поперечні перерізи фотоподілу ізоотопів ^{238,239,240,241,242,244}Pu теоретично розраховано за допомогою колективної напівкласичної моделі газу Фермі (CSCFGM) за допомогою комп'ютерного коду Talys у діапазоні енергій 1 - 30 МеВ. Густина ядерних рівнів має важливе значення для визначення структурних властивостей ядер. CSCFGM – це модель густини ядерних рівнів, що включає колективні (обертальні та вібраційні) ефекти, а також ефекти спарювання та оболонки, і використовується для аналізу реакцій (γ , f) ізоотопів плутонію. Експериментальні дані для всіх реакцій узяті з бібліотеки EXFOR. Теоретичні розрахунки узгоджуються з експериментальними даними, результатами за кодом Talys без зміни вхідних даних і оціненими даними ядерних поперечних перерізів із бібліотеки TENDL 2021.

Ключові слова: реакція фотоподілу, Talys, густина ядерних рівнів, ізоотопи плутонію.

Надійшла/Received 15.11.2021